AAPS PharmSciTech (2023) 24:95
https://doi.org/10.1208/s12249-023-02550-7

RESEARCH ARTICLE

Structural Changes in Liposomal Vesicles in Association with Sodium Taurodeoxycholate

Deepak Kumar[1] · Abhishek Suna[1] · Debes Ray[2] · Vinod K. Aswal[2] · Pratap Bahadur[3] · Sanjay Tiwari[1]

Received: 7 November 2022 / Accepted: 6 March 2023 / Published online: 3 April 2023

Abstract

Liposomes composed of soy lecithin (SL) have been studied widely for drug delivery applications. The stability and elasticity of liposomal vesicles are improved by incorporating additives, including edge activators. In this study, we report the effect of sodium taurodeoxycholate (STDC, a bile salt) upon the microstructural characteristics of SL vesicles. Liposomes, prepared by the thin film hydration method, were characterized by dynamic light scattering (DLS), small-angle neutron scattering (SANS), electron microscopy, and rheological techniques. We noticed a reduction in the size of vesicles with the incremental addition of STDC. Initial changes in the size of spherical vesicles were ascribed to the edge-activating action of STDC (0.05 to 0.17 μM). At higher concentrations (0.23 to 0.27 μM), these vesicles transformed into cylindrical structures. Morphological transitions at higher STDC concentrations would have occurred due to its hydrophobic interaction with SL molecules in the bilayer. This was ascertained from nuclear magnetic resonance observations. Whereas shape transitions underscored the deformability of vesicles in the presence of STDC, the consistency of bilayer thickness ruled out any dissociative effect. It was interesting to notice that SL-STDC mixed structures could survive high thermal stress, electrolyte addition, and dilution.

Keywords bile salt · edge activator · elasticity · liposomes · mixed vesicles · soy lecithin

Abbreviations

SL	Soy lecithin
STDC	Sodium taurodeoxycholate
MLV	Multilamellar vesicles
UL	Unilamellar vesicles
NMR	Nuclear magnetic resonance
HR-TEM	High-resolution transmission electron microscopy
PDI	Polydispersity index
D_h	Hydrodynamic diameter
PEG	Polyethylene glycol
DLS	Dynamic light scattering
SANS	Small angle neutron scattering

Introduction

Liposomes are formulated with phospholipid carrying the hydrophilic head and lipophilic tails. Their single- or multi-layered vesicular structure enables the incorporation of hydrophilic as well as hydrophobic payloads simultaneously. In accordance to polarity, such payloads occupy the hydrophilic core and hydrophobic bilayer region, respectively [1, 2]. Liposomes improve the therapeutic efficacy of drugs through the stabilization of molecules against degradation and the overcoming of physiological obstacles [3, 4]. Researchers have succeeded in co-delivering drugs and diagnostic substances which allows monitoring of the progression of therapy [5–7]. Apart from theranostics, charged liposomes have been developed for gene transfer applications. Several liposomal formulations have been approved by the US-FDA for clinical use, and others are under the advanced stage of trials [8]. The structure of liposomes can be tailored through changes in the composition and/or functionalization of phospholipids. This includes the incorporation of organic additives for improving the membrane characteristics (elasticity/deformability) [9], and a well-studied PEGylation strategy for steric stabilization and improving the circulation half-life of liposomes [10]. Elasticity

✉ Sanjay Tiwari
tiwarisanju@gmail.com

[1] Department of Pharmaceutics, National Institute of Pharmaceutical Education and Research (NIPER), Raebareli, Lucknow 226002, India

[2] Solid State Physical Division, Bhabha Atomic Research Centre, Mumbai 400085, India

[3] Department of Chemistry, Veer Narmad South Gujarat University, Surat, Gujarat 395007, India

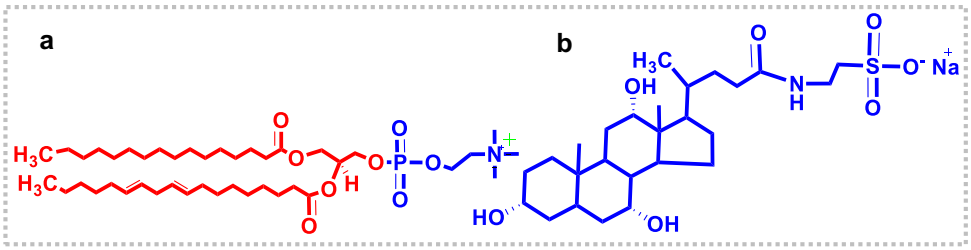

Fig. 1 Molecular structure of soy lecithin (**a**) and sodium taurodeoxycholate (**b**)

facilitates the transport of liposomes through the tough skin barrier and, thus, minimizes the requirement for penetration enhancers [11, 12].

The stability of liposomes is dictated by the rigidity of the bilayer membrane [13]. A sufficiently rigid bilayer protects the vesicles against fusion or dissociation under practical use conditions. At the same time, membrane rigidity dictates "on-demand" discharge of the payload from stimuli-responsive liposomes. Such formulations can be actuated by ultrasound, pulsed electromagnetic fields, and other external factors [14]. At the systemic level, the rigidity of liposomes has been shown to correlate with the response of regulatory T cells [15]. The literature suggests that bilayer rigidity can be modulated by the length and saturation of carbon chains of phospholipids. Mixing of lipids, particularly sterols, remains the most common approach and has given encouraging results. It works through the formation of interspersed rigid and fluid domains [16]. Recently, Lim and a coworker [17] demonstrated that cholesterol engages with poorly water-soluble drugs via hydrophobic forces and improves their loading. Such interactions contribute to achieving rate-controlled discharge kinetics from the formulations. The analogues of cholesterol such as stigmasterol, β-sitosterol, ergosterol, and lanosterol have also been employed for rigidization [18]. Charged derivatives interact more efficiently with phospholipid as a result of electrostatic forces operating in tandem with hydrogen bonding. Such an observation has been recorded for the dipalmitoylphosphatidylcholine-cholesteryl hemisuccinate mixture carrying quaternary ammonium and carboxylic acid groups, respectively [19]. Overall, interfacial properties of bilayer, and the shape, elasticity, and organization of a specific phospholipid are regulated by the presence of saturated and unsaturated groups in its structure. These properties can, therefore, be tailored through the incorporation of additives with suitable structural attributes [20].

Some groups have proposed the use of bile salts for the rigidization of the bilayer, keeping in view the instability of cholesterol-containing liposomes in gastrointestinal fluid. Bile salts consist of a short ionic chain linked to a rigid and slightly curved hydrophobic steroid moiety [21]. Physiologically, bile salt assists in the digestion and absorption of fats produced following lipolysis. By virtue of micellization potential and ability to alter the spontaneous curvature of self-assemblies, these biological amphiphiles are expected to form more stable association structures with phospholipids [22]. This is contrary to the disordered domains produced by cholesterol [15]. The interfacial action of bile salt facilitates the intestinal absorption of the formulation [23]. It is, therefore, pertinent to understand the phase behavior and dynamics of the bilayer during changes in the molar ratio of phospholipid and bile salt.

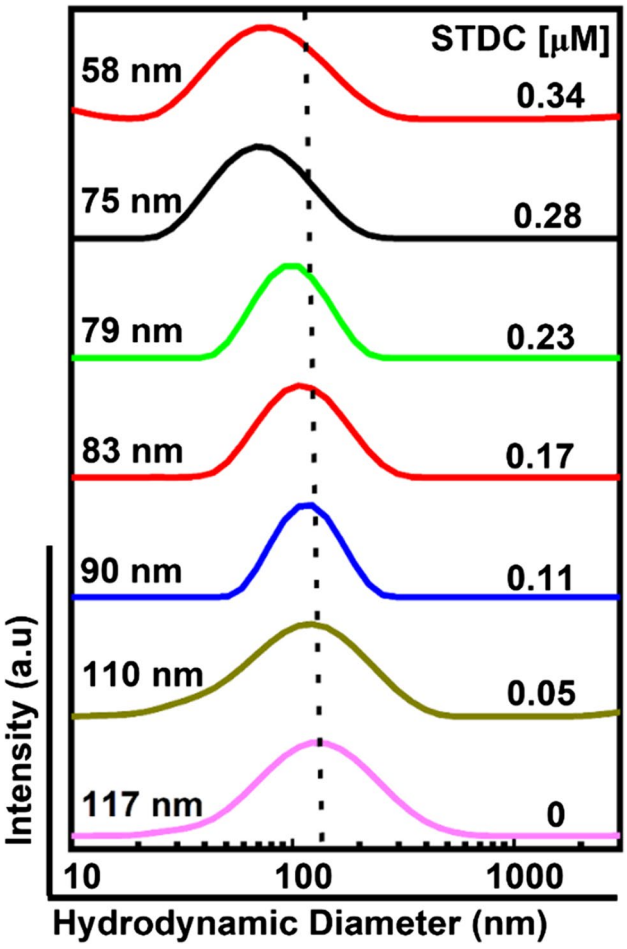

Fig. 2 Changes in hydrodynamic diameter of liposomal vesicles upon the incorporation of STDC at different concentrations

In this study, we look at newer assemblies emerging possibly at a different molar ratio of SL as phospholipid and sodium taurodeoxycholate (STDC) as bile salt. SL contains phosphatidylcholine, phosphatidylethanolamine, phosphatidylinositol, and phosphatidic acid and has been found to be biocompatible and biodegradable [24]. Vesicles, produced with the varying molar ratio of SL and STDC, were characterized using dynamic light scattering, electron microscopic, and rheological techniques. We delineate the threshold concentration of STDC at which morphological (sphere to cylinder) and structural (vesicle to mixed-micelle) transitions would occur. These observations can be used to rationalize the composition of liposomal formulations during drug delivery applications.

Materials and Methods

Materials

Soy lecithin (SL), sodium taurodeoxycholate hydrate (STDC) (Fig. 1), potassium dihydrogen phosphate, calcium chloride, and sodium chloride were purchased from Sisco Research Laboratories, India. Aluminum chloride was purchased from Thermo Fisher Scientific, India. Chloroform was purchased from Merck Life Science, India. Disodium hydrogen phosphate was purchased from Sigma Aldrich, USA. Deionized water was used for formulation development. A sample for small-angle neutron scattering experiments was prepared in heavy water (99.9% purity) and purchased from Sigma Aldrich, USA.

Methods and Characterizations

Preparation of Liposomes

Liposomes were prepared by the solvent evaporation method [25]. A total of seven batches were prepared as per the composition given in Table S1. The effect of STDC (0.05, 0.11, 0.17, 0.23, 0.28, and 0.34 μM) was investigated at a fixed concentration of SL (0.01 mM). The components were dissolved in chloroform (2 mL) which was later evaporated under reduced pressure. As produced, the film was hydrated in phosphate buffer (pH 7.4; 3 mL) under mild shaking to formulate vesicles. These vesicles were large (hydrodynamic size ~200 nm) and heterogeneous ($PDI > 0.36$). Narrowly distributed small-sized vesicles were prepared through probe sonication at 30% amplitude (pulse time: 10 s and resting time: 20 s). Three such cycles were performed. The dispersion was flushed with nitrogen, sealed, and stored at 4°C for further characterization.

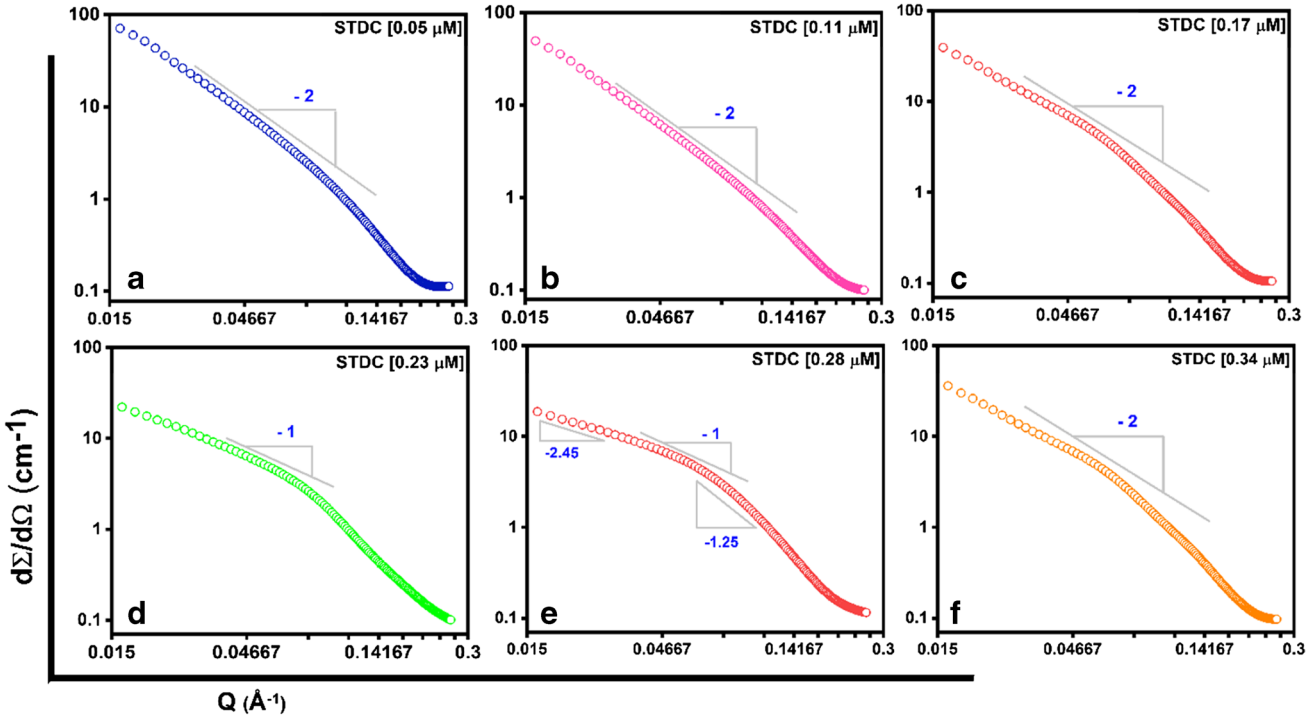

Fig. 3 Small-angle neutron scattering profile of liposomes showing the effect of STDC at increasing concentrations (**a-f**). The data were acquired at fixed temperature (30°C)

Table I Structural Parameters of Vesicles Calculated from the Fitted SANS Data

STDC, [μM]	Temperature (°C)	Structural parameters		Type of structure
0	25	$t_v \sim 27.8$ Å	$R_v > 400$ Å	Unilamellar vesicles
	30	$t_v \sim 27.3$ Å	$R_v > 400$ Å	Unilamellar vesicles
	40	$t_v \sim 27.1$ Å	$R_v > 400$ Å	Unilamellar vesicles
0.05	25	$t_v \sim 26.1$ Å	$R_v > 400$ Å	Unilamellar vesicles
	30	$t_v \sim 25.8$ Å	$R_v > 400$ Å	Unilamellar vesicles
	40	$t_v \sim 25.7$ Å	$R_v > 400$ Å	Unilamellar vesicles
0.11	25	$t_v \sim 21.9$ Å	$R_v > 400$ Å	Unilamellar vesicles
	30	$t_v \sim 21.3$ Å	$R_v > 400$ Å	Unilamellar vesicles
	40	$t_v \sim 22.1$ Å	$R_v > 400$ Å	Unilamellar vesicles
0.17	25	$t_v \sim 24.8$ Å	$R_v > 400$ Å	Unilamellar vesicles
	30	$t_v \sim 24.4$ Å	$R_v > 400$ Å	Unilamellar vesicles
	40	$t_v \sim 24.5$ Å	$R_v > 400$ Å	Unilamellar vesicles
0.23	25	$R_{cr} \sim 20.8$ Å	$L_r > 400$ Å	Rod-like micelles
	30	$R_{cr} \sim 21.8$ Å	$L_r > 400$ Å	Rod-like micelles
	40	$R_{cr} \sim 24.0$ Å	$L_r > 400$ Å	Rod-like micelles
0.28	25	$R_{cr} \sim 19.3$ Å	$L_r > 400$ Å	Rod-like micelles
	30	$R_{cr} \sim 19.3$ Å	$L_r > 400$ Å	Rod-like micelles
	40	$R_{cr} \sim 19.7$ Å	$L_r > 400$ Å	Rod-like micelles
0.34	25	$t_v \sim 24.0$ Å	$R_v > 400$ Å	Unilamellar vesicles
	30	$t_v \sim 23.9$ Å	$R_v > 400$ Å	Unilamellar vesicles
	40	$t_v \sim 23.9$ Å	$R_v > 400$ Å	Unilamellar vesicles

t_v, vesicle thickness; R_v, vesicle radius, R_{cr}, cross-sectional radius; L_r, length of rod; STDC, sodium taurodeoxycholate

Characterization of Liposomes

Hydrodynamic diameter (D_h), particle size distribution, and PDI were characterized by dynamic light scattering (Nano ZS, Malvern Instrument, UK). The samples were exposed to a laser (wavelength: 633 nm) and the data were acquired at a scattering angle of 173°. Zeta potential was recorded using deionized water as the dispersion medium. High-resolution transmission electron microscopy (HR-TEM) was used to visualize the morphology of vesicles using a field emission gun transmission electron microscope (Tecnai TF20, USA) with an accelerated voltage of 200 kV. The samples were dried over the grid and coated with copper prior to analysis.

The stability of the formulation was studied against temperature, dilution, and exposure to different electrolytes. It was challenged with commonly used mono-, bi-, and trivalent salts (NaCl, $CaCl_2$, and $AlCl_3$) at a fixed concentration of 0.9%.

Microstructural characterization of the formulation was performed by small-angle neutron scattering (SANS) experiments. The scattering intensity ($d\Sigma/d\Omega$) per unit volume was measured as a function of wave vector transfer Q ($=4\pi \sin\theta/\lambda$, whereas λ represents the wavelength of incident neutron and 2θ as the scattering angle). The mean neutron wavelength of 5.2 Å, with a resolution of $\Delta\lambda/\lambda$ ~15% from the neutron velocity selector, was used during the experiment. The angular distribution of scattered neutrons was performed by a one-dimensional position-sensitive detector. The data fitting and analyses were performed through SASfit software (supporting information).

Nuclear magnetic resonance (NMR) spectroscopy was performed on a JEOL spectrometer operating at 500 MHZ and equipped with a ROYAL HFX FGSQ probe. Spectra were processed using a JEOL Delta NMR processor (Ver.5.3.1). Rheological characterizations were carried out at 25°C using a rotational rheometer (Anton Paar, Austria). The data were analyzed using RheoCompass software. The experiments were performed using a cone plate (CP1/25). Viscoelastic behavior of the formulation was studied over a shear rate range of 0.1–100 Pa. During steady-shear measurements, sufficient time was allowed before acquisition at each shear rate to ensure that the viscosity reached its steady-state point.

Results and Discussion

Formulated liposomes were first investigated for particulate characteristics. The average hydrodynamic diameter (D_h) of initially hydrated liposomes was found to be 188 nm. High PDI highlights the heterogeneity in the vesicle population. We believe that heterogeneity arose from the formation of less organized structures during film hydration. One can notice multiple populations of vesicles (Table S1). We attribute it to the formation of multi-lamellar vesicles (MLVs) with $D_h > 300$ nm [26]. Downshift in D_h and *PDI* values can clearly be noticed upon: (a) sonication, and (b) incorporation of STDC into the dispersion (Fig. 2). Size reduction during sonication results from the dissociation of MLVs under cavitation stress. These are later organized more uniformly to produce unilamellar vesicles (ULVs). The formation of ULVs in the presence of STDC can be explained by taking into account its surface-active action. Analogous to the solubilization of lipid components in meals, STDC might have

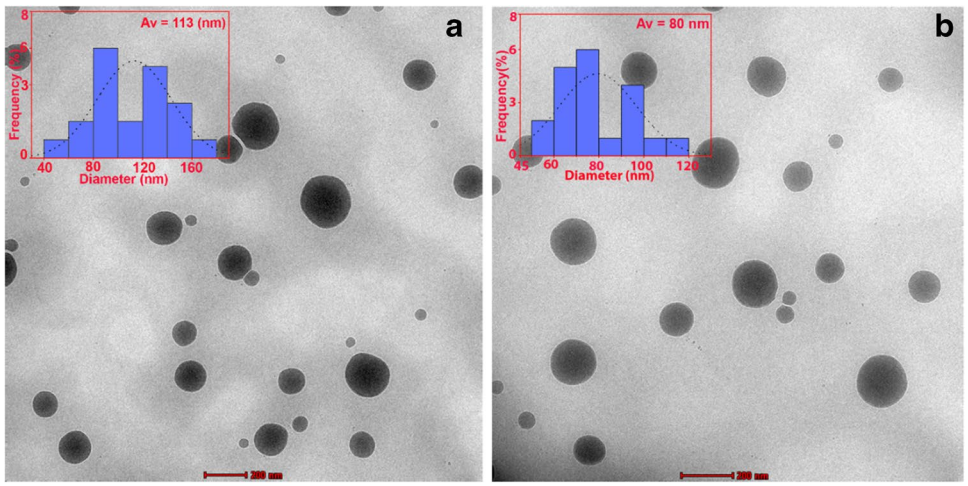

Fig. 4 High-resolution transmission electron microscopic image of liposomes without (**a**) and with STDC (**b**). The concentration of STDC in (**c**) is 0.28 µM. Scale bar: 200 nm

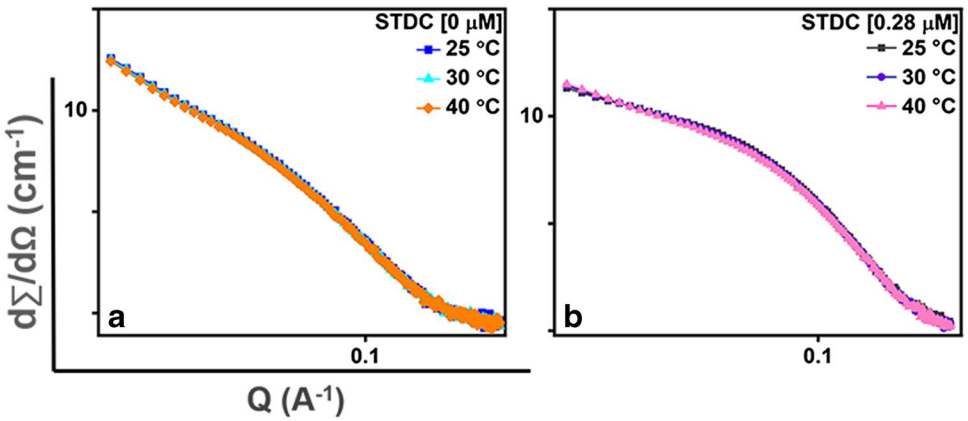

Fig. 5 Small-angle neutron scattering profile of liposomes showing the effect of temperature in neat SL (**a**) and SL-STDC mixed (**b**) vesicles

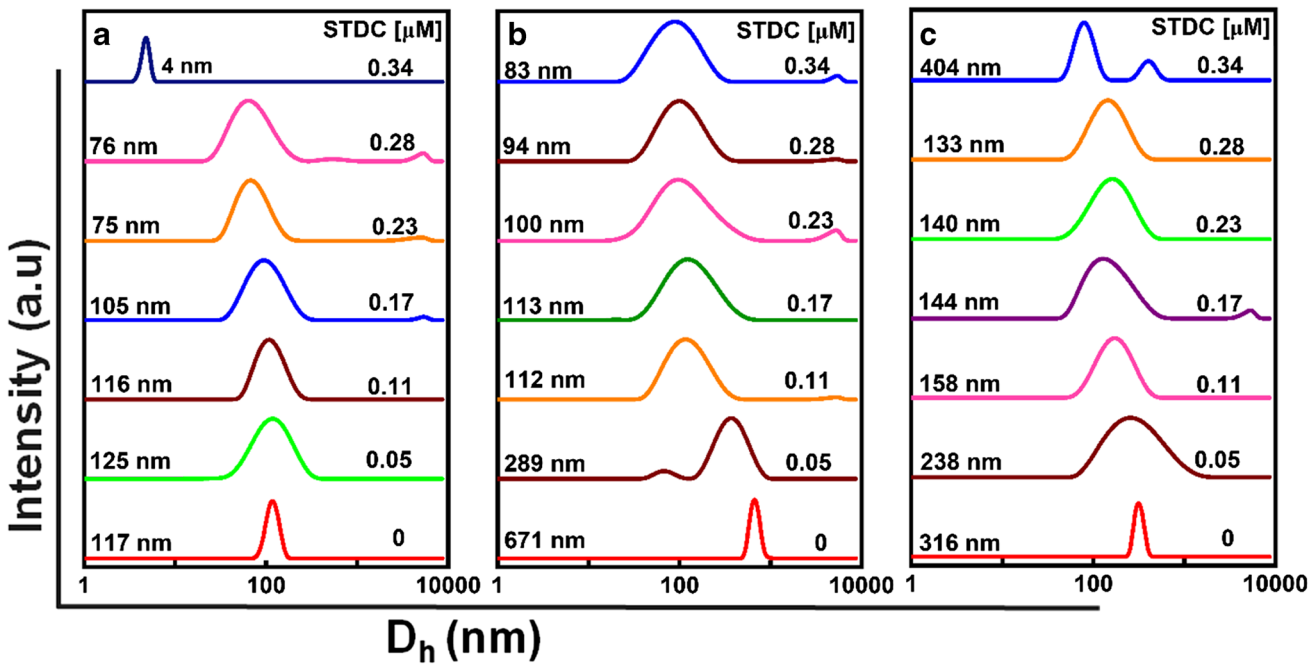

Fig. 6 Changes in the hydrodynamic diameter of neat soy lecithin and mixed vesicles in the presence of 0.9% NaCl (**a**), $CaCl_2$ (**b**), and $AlCl_3$ (**c**). Data were acquired at 30°C

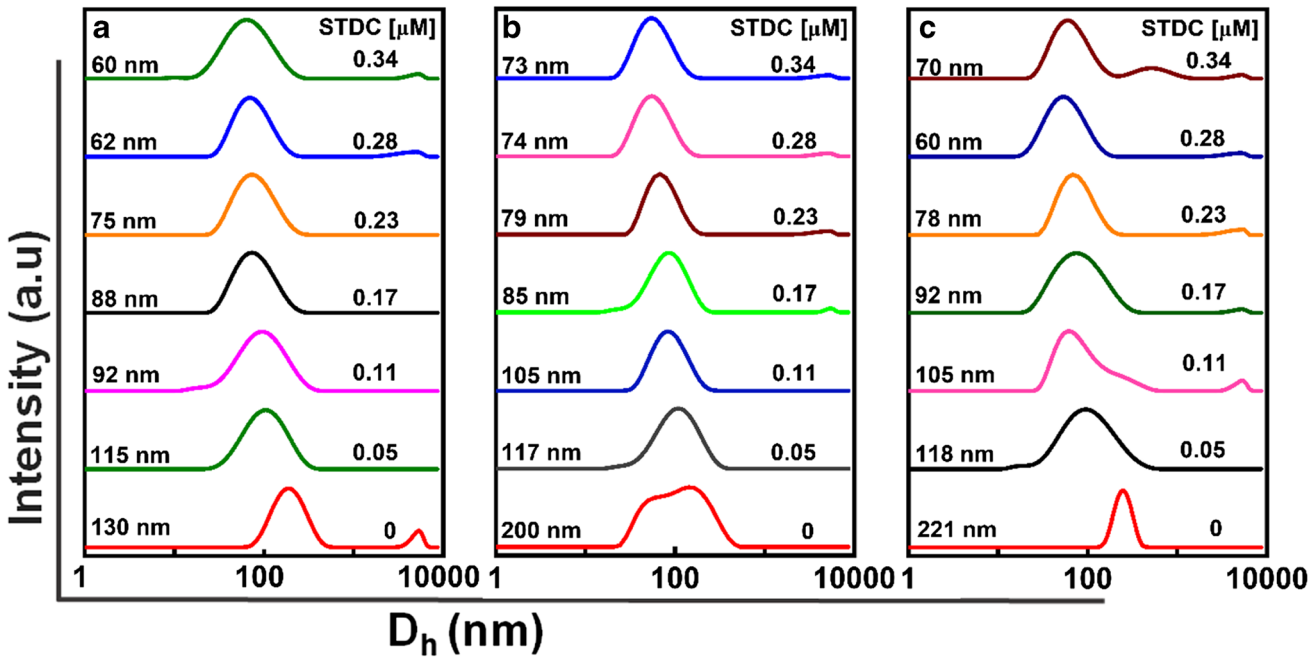

Fig. 7 Dilution stability soy lecithin vesicles in the presence of a different concentration of STDC. Data shown in **a**, **b,** and **c**, respectively, represent 10, 100, and 1000-fold dilution in water

caused dissociation of pre-existing phospholipid assembly [27]. Most likely, this gave an opportunity to STDC molecules in co-assembling with phospholipid.

Reduction in the size of mixed aggregates can be attributed to the edge-activating action of STDC on curvophobic phospholipid. It eventually affects the curvature of the bilayer [28, 29]. Changes in curvature create an opportunity for STDC molecules to undergo intercalation in the bilayer, as demonstrated by Mohapatra and Mishra [30]. In premicellar concentrations, bile salt molecules surrounded the bilayer and caused the hydration of liposomes deep until the core region. In our case, bile salts are partitioned into the bilayer without any disruptive events. This can be verified from the unimodality of the intensity peak in the dynamic light scattering data. A steady decline in the average size can be noticed. STDC molecules could reduce the surface tension of the vesicles in a concentration-dependent manner which explains the reduction in the diameter.

We now looked at the possibility of structural transformation and shape changes in vesicles during the above-mentioned reorganizations. Such transformations occur commonly in self-assembled structures during the incorporation of additives and have been studied extensively by our group on nonionic surfactants [31]. These transformations are driven by hydrophobic, electrostatic, van der Waals, and other non-specific forces. For instance, shape changes in charged micelles can simply be induced by increasing the ionic strength of the solution. Here, ionic strength correlates with changes in micellar dipoles [32].

Traces of shape change can be visualized in SANS data (Fig. 3a–f) plotted between scattering intensity ($d\Sigma/d\Omega$) and wave vector (Q). The derived parameters of these data are presented in Table I. Keeping together the numerical value of bilayer thickness (<5 nm) and hydrodynamic diameter (>40 nm), it becomes clear that the vesicles carried a single bilayer [33]. Fitted data suggest that unilamellar vesicles first transformed to rod-shaped core-shell structures (0.23 μM STDC) which were later re-arranged to attain spherical morphology (0.34 μM STDC). Although vesicles remained spherical in between 0.05 and 0.17 μM STDC, a steady reduction in thickness can be noticed, underscoring its edge-activating action. In spite of this, we did not find any evidence of vesicle dissociation in the presence of STDC. It appears that, at higher concentrations, STDC molecules intercalated through the bilayer and engaged hydrophobically with SL. Traces of interaction between SL and STDC can be visualized in ^{1}H NMR spectroscopy. The disappearance of the peak corresponding to the steroidal ring (1–2 ppm) can be ascribed to the insertion of STDC in the bilayer (Fig. S1).

Similar observations have been recorded by other researchers as well [34]. It is worth mentioning that the extent of insertion (and hence their effect on bilayer fluidity) would depend upon the lipophilicity of specific bile salt. Micelles, another class of self-assemblies with a wide pharmaceutical interest, tend to swell and dissociate during the insertion of bile salts in the corona region [22].

The reflection of STDC-induced structural changes can be visualized in the neutron scattering profile. Apart from

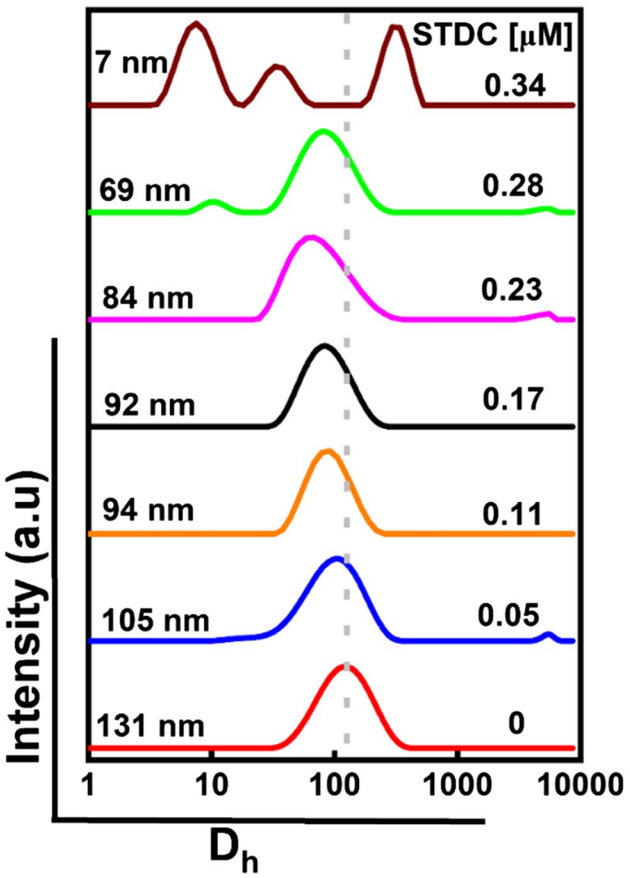

Fig. 8 Effect of autoclaving (121°C; 20 min; 18 *psi*; three cycles) upon size distribution of vesicles

a slight reduction in the scattering intensity, a weak hump formation can be noticed in the intermediate Q-region (0.04 to 0.14 Å) of the correlation peak among vesicles carrying 0.23 and 0.28 μM STDC. The unilamellarity of vesicles can be confirmed by the nature of peaks. For example, the hump in our case appears clearly suppressed and differs from the Bragg peak originating from large multilamellar vesicles (MLVs) [31]. Large MLVs show Q^{-4} dependence of a decline in scattering intensity [35]. We rule out structural or shape changes among vesicles exposed with STDC concentration less than 0.23 μM. This can also be attested from Q^{-2}-dependent decline in the scattering intensity of these samples (Fig. 3a–c). At higher concentration, the decline followed Q^{-1}-dependence suggesting that spherical vesicles transformed into cylindrical ones. The nature of slopes at 0.28 μM STDC hints towards the co-existence of spherical and cylindrical structures. This sample was, however, dominated by the cylinders which later converted to spherical vesicles (Fig. 3d–f).

We get a clearer evidence of the effect of STDC upon the size of vesicles while looking at HR-TEM data. The image reveals that spherical vesicles showed a decrease in diameter as STDC concentration increased. For instance, pure SL vesicles showed an average diameter of 113 nm which reduced to 80 nm in the presence of 0.28 μM STDC (Figs. 4a, b; S2). Some groups have reported complete rupture of vesicles and solubilization of lipids depending upon the partition behavior of the surfactants. Some of these can flip to the inner monolayer and trigger rapid solubilization. Contrarily, the action of weaker surfactants may remain confined to the edge or interlayers [36]. In the latter case, vesicular intermediates and mixed assemblies are formed, as observed in our formulation.

The effect of edge-activation was investigated upon the stability of the formulation against dispersion temperature, ionic strength, and dilution was also investigated. SANS data attest to the stability of mixed vesicles until 40°C; we did not observe any changes in neutron scattering (Fig. 5a, b; S3).

Similarly, vesicles remained stable at pH 5 and 8 (Fig. S4). Next, the stability of formulation was challenged with commonly used mono-, bi-, and trivalent salts (NaCl, $CaCl_2$, and $AlCl_3$) at a fixed concentration of 0.9% (Fig. 6a–c). These ions are present in biological systems and serve important physiological roles at cellular and extracellular levels. In line with previous reports, NaCl did not affect the stability of mixed vesicles carrying up to 0.28 mM STDC. This is probably the reason of co-encapsulating NaCl as high as 0.7 M for making liposomes responsive to microwave irradiation during the elimination of solid tumors. Here, the NaCl acts as a thermo-seed and causes a rapid elevation in temperature at the tumor site [37, 38].

Stabilizing effect of STDC is clearly evident among vesicles exposed to $CaCl_2$ and $AlCl_3$ which caused a high upshift in size (more than five- and two-fold increase, respectively) in neat SL vesicles. The data on the average size and PDI indicate that vesicles became more organized in the presence of STDC (Table S2). A steady drop in the size and PDI occurred in these samples at increasing concentrations of STDC. This can be ascribed to the fusion and/or aggregation of vesicles as a result of dehydration and charge-neutralization caused by multivalent cations [39, 40]. This is analogous to the effect of electrolytes upon water structures around the shell of polyoxyethylene-polyoxypropylene–based block copolymeric micelles studied extensively by our group [41, 42]. In addition to its direct action on the bilayer, the protective effect of anionic STDC lies in its ability to capture cations and form neutral salt [43]. Similar arguments have been given by McClements and coworkers to explain the electrostatic interaction between taurocholate and polylysine [44].

Our data suggest that neat SL vesicles could not withstand dilution, even up to tenfold. This is verifiable from the appearance of multi-modality in the vesicle population and the loss of symmetry in the primary peak. As opposed to this, mixed vesicles retained their stability even after

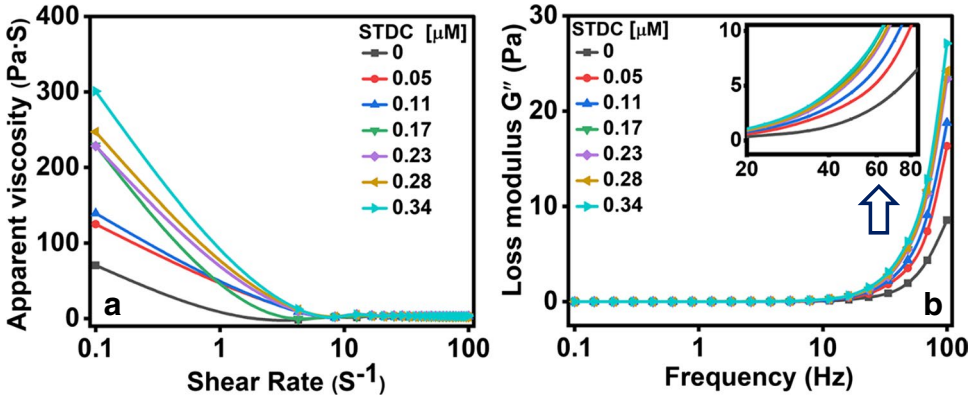

Fig. 9 Changes in the viscosity of liposomal dispersion at increasing concentration of STDC (**a**). The data of loss modulus (G″) for these compositions are shown (**b**). The experiments were performed at 25°C

1,000-fold dilution (Fig. 7a–c). For example, those carrying 0.23 μM STDC showed identical distribution profile (D_h = 75–79 nm; *PDI* = 0.183–0.233) regardless of the extent of dilution.

Importantly, the mixed vesicular dispersion was found to be stable during three cycles of autoclaving (121°C; 20 min; 18 *psi*). Such a high temperature offers high mobility to the bilayer components and creates an opportunity for the dissociation of vesicles [45]. We, however, did not notice any turbidity or other physical signs of destabilization in the dispersion. It highlights the fact that bilayers were not ruptured under the high thermal stress typically applied during the sterilization of injectable formulations (Fig. 8).

We noticed that mixed vesicles containing 0.34 μM STDC behaved differently when challenged with salt addition and thermal stress (Figs. 6 and 8). This can probably be related to the high edge-activating action of STDC at this concentration traces of which are visible in Fig. 2. We argue that the destabilization would have been contributed by the salts through alteration in water clusters in the vicinity of the interface. Similarly, these vesicles could not withstand the stress of an autoclaving cycle.

Our data at low shear rate highlight two important points: (a) steady increase in the viscosity of dispersion with an increase in STDC concentration, and (b) thinning of dispersion at higher shear rates (0.5 to 5 s^{-1}). The first point can be understood, taking into account the shape changes stimulated by STDC (Fig. 9a). Dispersions containing elongated or a mixture of elongated and spherical vesicles offer greater opportunities of engagement. It translates into the viscous behavior of existing structures [46]. This is analogous to the superior entanglement density of hydrophilic colloids which later form weak association structures [47].

Viscoelastic properties of these dispersions were ascertained through oscillatory measurements. Here, loss or viscous modulus (G″) was recorded as a function of oscillation frequency (ω). The frequency dependence of samples increased marginally at increasing STDC concentration. Furthermore, G″ values of all samples remained lower than G′ which attests elastic behavior of vesicles (Fig. S5). Altogether, rheology data ascertain the viscoelastic behavior of mixed vesicles (Fig. 9b). Tung and coworkers [48] have reported that in systems formulated with a higher concentration of lecithin, the incorporation of negatively charged bile salts causes strong repulsion in bilayers. This offers the opportunity of developing a series of phases (viscoelastic, gel-like, and low-viscosity fluids) and architectures by tuning the molar ratio of phospholipid to bile salt.

Conclusion

We have successfully demonstrated that STDC stabilizes vesicles composed of SL and modulates their microstructural characteristics. Our interpretations are based on the findings of scattering and rheological experiments. We show that initially formed unilamellar spherical vesicles underwent a transition to cylindrical and spherical structures depending upon the concentration of STDC. We attribute these changes to the edge-activating action of STDC at the interface at low concentration (0.05 to 0.17 μM). At higher concentration, STDC molecules engaged hydrophobically with the phospholipid to form mixed structures. We assert that morphological transitions were driven by these hydrophobic interactions. Improvement in the viscoelastic behavior, deformability, and stability of vesicles in the presence of STDC is interesting from the viewpoint of their application in drug loading and delivery.

Supplementary Information The online version contains supplementary material available at https://doi.org/10.1208/s12249-023-02550-7.

Acknowledgements ST acknowledges the Central Instrument Facility of NIPER-Raebareli and CRF IIT-Delhi for NMR and HR-TEM data collection.

Author Contribution Deepak Kumar and Abhishek Suna: investigation, writing—original draft. Debes Ray and V.K. Aswal: formal analysis—SANS data. Pratap Bahadur: writing—review and editing. Sanjay Tiwari: conceptualization, writing—review and editing, and project administration.

Funding DK and AS thank the Ministry of Chemicals and Fertilizers (Govt. of India) for providing the fellowship to carry out this research, communication no.: NIPER-R/397.

Data Availability Data will be made available on request.

Declarations

Conflict of Interest The authors declare no competing interests.

References

1. Rehman AU, Omran Z, Anton H, Mely Y, Akram S, Vandamme TF, et al. Development of doxorubicin hydrochloride loaded pH-sensitive liposomes: investigation on the impact of chemical nature of lipids and liposome composition on pH-sensitivity. Eur J Pharm Biopharm. 2018;133:331–8.
2. Lu B, Ma Q, Zhang J, Liu R, Yue Z, Xu C, et al. Preparation and characterization of bupivacaine multivesicular liposome: a QbD study about the effects of formulation and process on critical quality attributes. Int J Pharm. 2021;598:120335.
3. Guimaraes D, Cavaco-Paulo A, Nogueira E. Design of liposomes as drug delivery system for therapeutic applications. Int J Pharm. 2021;601:120571.
4. Wang C, Xiao J, Hu X, Liu Q, Zheng Y, Kang Z, et al. Liquid core nanoparticle with high deformability enables efficient penetration across biological barriers. Adv Healthc Mater. 2023;12:2201889.
5. Li S, Goins B, Zhang L, Bao A. Novel multifunctional theranostic liposome drug delivery system: construction, characterization, and multimodality MR, near-infrared fluorescent, and nuclear imaging. Bioconjug Chem. 2012;23:1322–32.
6. Celia C, Cristiano MC, Froiio F, Di Francesco M, d'Avanzo N, Di Marzio L, et al. Nanoliposomes as multidrug carrier of gemcitabine/paclitaxel for the effective treatment of metastatic breast cancer disease: a comparison with gemzar and taxol. Adv Therap. 2021;4:2000121.
7. Xu S, Zhang P, Heing-Becker I, Zhang J, Tang P, Bej R, et al. Dual tumor-and subcellular-targeted photodynamic therapy using glucose-functionalized MoS_2 nanoflakes for multidrug-resistant tumor ablation. Biomaterials. 2022;290:121844.
8. Crommelin DJA, Van Hoogevest P, Storm G. The role of liposomes in clinical nanomedicine development. What now? Now what? J Control Release. 2020;318:256–63.
9. Szabova J, Misik O, Havlikova M, Lizal F, Mravec F. Influence of liposomes composition on their stability during the nebulization process by vibrating mesh nebulizer. Colloids Surf B Biointerfaces. 2021;204: 111793.
10. Awad NS, Paul V, Mahmoud MS, Al Sawaftah NM, Kawak PS, Al Sayah MH, et al. Effect of pegylation and targeting moieties on the ultrasound-mediated drug release from liposomes. ACS Biomater Sci Eng. 2020;6:48–57.
11. Sudhakar K, Mishra V, Jain S, Rompicherla NC, Malviya N, Tambuwala MM. Development and evaluation of the effect of ethanol and surfactant in vesicular carriers on lamivudine permeation through the skin. Int J Pharm. 2021;610:121226.
12. Barone A, Cristiano MC, Cilurzo F, Locatelli M, Iannotta D, Di Marzio L, et al. Ammoniumglycyrrhizate skin delivery from ultradeformable liposomes: a novel use as anti-inflammatory agent in topical drug delivery. Colloids Surf B Biointerfaces. 2020;193: 111152.
13. Liang X, Mao G, Ng KYS. Mechanical properties and stability measurement of cholesterol-containing liposome on mica by atomic force microscopy. J Colloid Interface Sci. 2004;278:53–62.
14. Trilli J, Caramazza L, Paolicelli P, Casadei MA, Liberti M, Apollonio F, et al. The impact of bilayer rigidity on the release from magnetoliposomes vesicles controlled by PEMFs. Pharmaceutics.2021;13:1712.
15. Benne N, Leboux RJT, Glandrup M, van Duijn J, Lozano Vigario F, Neustrup MA, et al. Atomic force microscopy measurements of anionic liposomes reveal the effect of liposomal rigidity on antigen-specific regulatory T cell responses. J Control Release. 2020;318:246–55.
16. Mouritsen OG, Jorgensen K. Dynamical order and disorder in lipid bilayers. Chem Phys Lipids. 1994;73:3–25.
17. Lim E-B, Haam S, Lee S-W. Sphingomyelin-based liposomes with different cholesterol contents andpolydopamine coating as a controlled delivery system. Colloids Surf A Physicochem Eng Asp. 2021;618:126447.
18. Cui M, Wu W, Hovgaard L, Lu Y, Chen D, Qi J. Liposomes containing cholesterol analogues of botanical origin as drug delivery systems to enhance the oral absorption of insulin. Int J Pharm. 2015;489:277–84.
19. Ding WX, Qi XR, Li P, Maitani Y, Nagai T. Cholesteryl hemisuccinate as a membrane stabilizer in dipalmitoylphosphatidylcholine liposomes containing saikosaponin-d. Int J Pharm. 2005;300:38–47.
20. Van den Bergh BA, Wertz PW, Junginger HE, Bouwstra JA. Elasticity of vesicles assessed by electronspin resonance, electron microscopy and extrusion measurements. Int J Pharm. 2001;217:13–24.
21. Zhang S, Wang X. Effect of vesicle-to-micelle transition on the interactions of phospholipid/sodium cholate mixed systems with curcumin in aqueous solution. J Phy Chem B. 2016;120:7392–400.
22. Rathod S, Joshi A, Ray D, Aswal VK, Verma G, Bahadur P, et al. Changes in aggregation properties of TPGS micelles in the presence of sodium cholate. Colloids Surf A Physicochem Eng Asp. 2021;610:125938.
23. Niu M, Lu Y, Hovgaard L, Guan P, Tan Y, Lian R, et al. Hypoglycemic activity and oral bioavailability of insulin-loaded liposomes containing bile salts in rats: the effect of cholate type, particle size and administered dose. Eur J Pharm Biopharm. 2012;81:265–72.
24. Kafle A, Akamatsu M, Bhadani A, Sakai K, Kaise C, Kaneko T, et al. Phase behavior of the bilayers containing hydrogenated soy lecithin and β-sitosteryl sulfate. Langmuir. 2020;36:6025–32.
25. Zhang X, Lei B, Wang Y, Xu S, Liu H. Dual-sensitive on–off switch in liposome bilayer for controllable drug release. Langmuir. 2019;35:5213–20.
26. Touti R, Noun M, Guimberteau F, Lecomte S, Faure C. What is the fate of multi-lamellar liposomes of controlled size, charge and elasticity in artificial and animal skin? Eur J Pharm Biopharm. 2020;151:18–31.
27. Lichtenberg D, Ahyayauch H, Goni FM. The mechanism of detergent solubilization of lipid bilayers. Biophys J. 2013;105:289–99.
28. Lee EH, Kim A, Oh Y-K, Kim C-K. Effect of edge activators on the formation and transfection efficiency of ultradeformable liposomes. Biomaterials. 2005;26:205–10.
29. Zhang Y, Shen L, Zhang K, Guo T, Zhao J, Li N, et al. Enhanced antioxidation via encapsulation of isooctyl p-methoxycinnamate with sodium deoxycholate-mediated liposome endocytosis. Int J Pharm. 2015;496:392–400.
30. Mohapatra M, Mishra AK. Effect of submicellar concentrations of conjugated and unconjugated bile salts on the lipid bilayer membrane. Langmuir. 2011;27:13461–7.
31. Rathod S, Arya S, Shukla R, Ray D, Aswal VK, Bahadur P, et al. Investigations on the role of edge activator upon structural transitions in span vesicles. Colloids Surfaces A Physicochem Eng Asp. 2021;627:127246.

32. Debye P, Anacker EW. Micelle shape from dissymmetry measurements. J Phys Chem. 1951;55:644–55.
33. Agrawal NR, Omarova M, Burni F, John VT, Raghavan SR. Spontaneous formation of stable vesicles and vesicle gels in polar organic solvents. Langmuir. 2021;37:7955–65.
34. Yang L, Tucker IG, Ostergaard J. Effects of bile salts on propranolol distribution into liposomes studied by capillary electrophoresis. J Pharm Biomed Anal. 2011;56:553–9.
35. Prameela G, Kumar BP, Reddy RR, Pan A, Subramanian J, Kumar S, et al. Vesicle to micelle transition in the ternary mixture of L121/SDS/D_2O: NMR, EPR and SANS studies. Phys Chem Chem Phys. 2017;19:31747–55.
36. Celino M. Biomembrane solubilization mechanism by Triton X-100: a computational study of the three stage model. 2017;19:29780–94.
37. Zhou Q, Wu S, Gong N, Li X, Dou J, Mu M, Yu X, Yu J, Liang P. Liposomes loading sodium chloride as effective thermo-seeds for microwave ablation of hepatocellular carcinoma. Nanoscale. 2017;9:11068–76.
38. Jin Y, Liang X, An Y, Dai Z. Microwave-triggered smart drug release from liposomes co-encapsulating doxorubicin and salt for local combined hyperthermia and chemotherapy of cancer. Bioconjug Chem. 2016;27:2931–42.
39. Dobrzynska I. Association equilibria of divalent ions on the surface of liposomes formed from phosphatidylcholine. Eur Phys J E. 2019;42:1–6.
40. Kotynska J, Figaszewski ZA. Binding of trivalent metal ions (Al^{3+}, In^{3+}, La^{3+}) with phosphatidylcholine liposomal membranes investigated by microelectrophoresis. Eur Phys J E. 2018;41:1–6.
41. Tiwari S, Singh K, Marangoni DG, Bahadur P. Amphiphilic star block copolymer micelles in saline as effective vehicle for quercetin solubilization. J Mol Liq. 2022;345:118259.
42. Patidar P, Bahadur A, Prasad K, Tiwari S, Aswal VK, Bahadur P. Synthesis, self-assembly and micellization characteristics of choline alkanoate ionic liquids in association with a star block copolymer. Colloids Surf A Physicochem Eng Asp. 2018;555:691–8.
43. Moore EW, Celic L, Ostrow JD. Interactions between ionized calcium and sodium taurocholate: bile salts are important buffers for prevention of calcium-containing gallstones. Gastroenterology. 1982;83:1079–89.
44. Lopez-Pena C, Arroyo-Maya IJ, McClements DJ. Interaction of a bile salt (sodium taurocholate) with cationic (ε-polylysine) and anionic (pectin) biopolymers under simulated gastrointestinal conditions. Food Hydrocoll. 2019;87:352–9.
45. Gou J, Chao Y, Liang Y, Zhang N, He H, Yin T, et al. Humid heat autoclaving of hybrid nanoparticles achieved by decreased nanoparticle concentration and improved nanoparticle stability using medium chain triglycerides as a modifier. Pharm Res. 2016;33:2140–51.
46. Yalcinkaya H, Feoktystov A, Gradzielski M. Formation of well-defined vesicles by styrene addition to a nonionic surfactant and their polymerization leading to viscous hybrid systems. Langmuir. 2018;34:9184–94.
47. Wang X, Liu L, Xia S, Muhoza B, Cai J, Zhang X, et al. Sodium carboxymethyl cellulose modulates the stability of cinnamaldehyde-loaded liposomes at high ionic strength. Food Hydrocoll. 2019;93:10–8.
48. Cheng C-Y, Wang T-Y, Tung S-H. Biological hydrogels formed by swollen multilamellar liposomes. Langmuir. 2015;31:13312–20.